Photosynthesis Research
https://doi.org/10.1007/s11120-022-00962-3

ORIGINAL ARTICLE

Removal of redox-sensitive Rubisco Activase does not alter Rubisco regulation in soybean

Christopher M. Harvey[1] · Amanda P. Cavanagh[2,3] · Sang Yeol Kim[4] · David A. Wright[5] · Ron G. Edquilang[2,6] · Kayla S. Shreeves[6] · Juan Alejandro Perdomo[2,7] · Martin H. Spalding[5] · Donald R. Ort[2,6] · Carl J. Bernacchi[1,2,6] · Steven C. Huber[1,6]

Received: 3 May 2022 / Accepted: 9 September 2022

Abstract

Rubisco activase (Rca) facilitates the catalytic repair of Rubisco, the CO_2-fixing enzyme of photosynthesis, following periods of darkness, low to high light transitions or stress. Removal of the redox-regulated isoform of Rubisco activase, Rca-α, enhances photosynthetic induction in *Arabidopsis* and has been suggested as a strategy for the improvement of crops, which may experience frequent light transitions in the field; however, this has never been tested in a crop species. Therefore, we used RNAi to reduce the Rca-α content of soybean (*Glycine max* cv. Williams 82) below detectable levels and then characterized the growth, photosynthesis, and Rubisco activity of the resulting transgenics, in both growth chamber and field conditions. Under a 16 h sine wave photoperiod, the reduction of Rca-α contents had no impact on morphological characteristics, leaf expansion rate, or total biomass. Photosynthetic induction rates were unaltered in both chamber-grown and field-grown plants. Plants with reduced Rca-α content maintained the ability to regulate Rubisco activity in low light just as in control plants. This result suggests that in soybean, Rca-α is not as centrally involved in the regulation of Rca oligomer activity as it is in *Arabidopsis*. The isoform stoichiometry supports this conclusion, as Rca-α comprises only ~ 10% of the Rubisco activase content of soybean, compared to ~ 50% in *Arabidopsis*. This is likely to hold true in other species that contain a low ratio of Rca-α to Rca-ß isoforms.

Keywords Rubisco activase · Soybean · Photosynthetic induction · Gas exchange · Western blot

Abbreviations

Φ	Photosynthetic quantum yield at low light (mmol CO_2 mol $PPFD^{-1}$)
A_{max}	Light saturated CO_2 assimilation rate (μmol m^{-2} s^{-1})
I_{50}	Irradiance at which assimilation is half of A_{max} (μmol m^{-2} s^{-1})
τ_s	Rubisco activation rate constant (min)
A_i	Initial carboxylation capacity during induction (μmol m^{-2} s^{-1})
A^*_f	Maximal carboxylation capacity achieved during induction (μmol m^{-2} s^{-1})
V_{cmax}	CO_2 saturated Rubisco carboxylation capacity (μmol m^{-2} s^{-1})
J_{max}	CO_2 saturated photosynthetic electron transport rate (μmol m^{-2} s^{-1})
R_d	Mitochondrial respiration rate in the light (μmol m^{-2} s^{-1})

✉ Christopher M. Harvey
cmharvey12675@gmail.com

1 Agricultural Research Service, Global Change and Photosynthesis Research Unit, United States Department of Agriculture, Urbana, IL, USA

2 Carl R. Woese Institute for Genomic Biology, University of Illinois at Urbana-Champaign, Urbana, IL, USA

3 School of Life Sciences, University of Essex, Colchester CO4 3SQ, UK

4 INARI Agriculture Inc, West Lafayette, IN, USA

5 Department of Genetics, Development and Cell Biology, Iowa State University, Ames, IA, USA

6 Departments of Plant Biology and Crop Sciences, University of Illinois at Urbana-Champaign, Urbana, IL, USA

7 School of Pharmacy and Biomedical Sciences, University of Central Lancashire, Preston PR1 2HE, UK

Published online: 27 September 2022

Introduction

The slow response of photoprotection, Ribulose-1,5-bisphosphate carboxylase/oxygenase (Rubisco) activity and stomatal conductance to abrupt light transitions is predicted to be a major source of lost crop productivity (Taylor and Long 2017; Slattery et al. 2018). Although field crops are grown in full sunlight, diurnal changes in sun angle, passing clouds and wind driven changes in self-shading of understories leads to regular and rapid changes in irradiation. In a simulated field wheat canopy, instantaneous and perfect adaptation to light transitions was predicted to improve diurnal carbon gain by 20% (Taylor and Long 2017). Improving the speed of this response is therefore a major objective of current research (Ort et al. 2015; Wang et al. 2020). Following high to low light transitions, photosynthesis is constrained by the slow relaxation of photoprotective dissipative energy processes known as non-photochemical quenching. Overexpression of three proteins involved in moderating non-photochemical quenching resulted in faster adaptation to fluctuating light and an increase in growth rate in *Nicotiana tabacum* (Kromdijk et al. 2016). This growth enhancement strategy does not work in all species, as it caused a decrease in biomass when tested in *Arabidopsis* (Garcia-Molina and Leister 2020). Following low to high light transitions, photosynthesis is primarily constrained by the activation of Rubisco (Soleh et al. 2017; Wang et al. 2020). Dynamic light conditions also require continuous adjustments of stomatal aperture in order to balance carbon gain against water loss which can be disturbed by delayed stomatal response (Lawson and Blatt 2014; Taylor and Long 2017; Slattery et al. 2018).

Rubisco catalyzes both the carboxylation and oxygenation of ribulose-1,5-bisphosphate (RuBP). Catalysis by Rubisco is error-prone and occasionally generates transition state analogs, such as xylulose-1,5-bisphosphate or 2,3-pentodiulose-1,5-bisphosphate, which tightly bind to and inhibit Rubisco's own active sites (Hauser et al. 2015). Rubisco may also be inhibited by the binding of various sugar phosphates, including substrate RuBP, to non-carbamylated (and thus inactive) active sites (Parry et al. 2008). These inhibitors must dissociate before activity can be restored. Uncatalyzed dissociation is very slow, and would lead to the accumulation of inactive Rubisco if not for the action of Rubisco activase (Rca). Rca uses the energy from ATP hydrolysis to remodel the active site of Rubisco and promote dissociation of inhibitory sugar phosphates (Hayer-Hartl 2017).

Rca is critical for the reactivation of Rubisco following low to high light transitions, and the rate of photosynthetic induction scales linearly with activase content (Mott et al. 1997; Hammond et al. 1998). Unfortunately, the amount of Rca and Rubisco present in a cell are negatively correlated (Mate et al. 1993; He et al. 1997; Fukayama et al. 2012), which may limit Rca overexpression as a viable means to enhance the rate of photosynthetic induction in crops. Removal of the redox-sensitive α isoform of Rca (Rca-α) may be a way to enhance photosynthetic induction without decreasing Rubisco content. Rca-α is expressed in many plant species alongside the shorter, redox insensitive ß isoform of Rca (Rca-ß), which is present in all plants. The two isoforms are highly conserved, but Rca-α has a C-terminal extension containing two redox sensitive cysteines. The comparative midpoint potentials of these Rca-α cysteines to those of thioredoxin-f (Hutchison et al. 2000) allows for large changes in the oxidized/reduced ratio of Rca-α from low to high light intensity similar to that of other thioredoxin-f regulated photosynthesis related enzymes that are largely oxidized under low to moderate light but become nearly fully reduced under high light (Hutchison et al. 2000; Yoshida et al. 2015). This light-dependent redox modulation of the C-terminal cysteines contributes to ADP-inhibition of mixtures of the two *Arabidopsis* isoforms (Zhang and Portis 1999). Thus, in *Arabidopsis*, the C-terminal extension of Rca-α allows an additional level of redox-dependent regulation that helps to limit ATP usage under low photosynthetically active radiation. In *Arabidopsis* the two isoforms are generated by alternative splicing of the same mRNA, while in soybean they are encoded by different genes. Removal of Rca-α from *Arabidopsis* caused photosynthesis to induce much more rapidly than in wildtype (Carmo-Silva and Salvucci 2013), but this result has yet to be tested in any other species.

Altering Rca contents could affect the thermal stability of photosynthesis. Rca is heat labile, and its denaturation is a major limitation of heat-stressed photosynthesis (Crafts-Brandner and Salvucci 2000; Salvucci et al. 2006; Ristic et al. 2009; Carmo-Silva et al. 2012; Carmo-Silva and Salvucci 2012), alongside disordering of the photosynthetic electron transport chain (Wise et al. 2004; Kubien and Sage 2008; Sage et al. 2008; Yamori and von Caemmerer 2009). Therefore higher Rca contents, either from prolonged heat stress or transgene overexpression, tend to enhance the thermotolerance of photosynthesis (DeRidder et al. 2012; Zhao et al. 2017; Scafaro et al. 2019a; Degen et al. 2020, 2021). This may be one reason why plants often possess more Rca than is necessary to maintain steady-state photosynthesis, as large (≥ 80%) reductions in Rca are necessary to decrease steady-state photosynthesis in most plants (Mate et al. 1996; Eckardt et al. 1997), but likely greatly slow photosynthesis in low to high light transitions. The C-terminal extension of Rca-α, in particular, may enhance protein thermal stability, as Rca oligomers containing Rca-α remained stable

at higher temperatures than oligomers composed solely of Rca-ß (Keown and Pearce 2014). In C4 grass species, Rca-α expression is induced only at high temperature resulting in higher Rubisco activation and higher photosynthesis under thermal stress (Kim et al. 2021).

In *Arabidopsis,* the removal of Rca-α led to much faster photosynthetic induction (Carmo-Silva and Salvucci 2013). Removal of Rca-α would therefore seem to be a viable strategy for enhancing the rate of photosynthetic induction without entailing a penalty to the rate of steady-state photosynthesis at least under near optimal growth temperatures. However, it is not clear whether this result is generally applicable, as the distribution of Rca-α is not universal, and many species express Rca-α at lower levels than *Arabidopsis*. In this study, we generated and characterized a novel set of transgenic soybean plants that containing reduced amounts of Rca-α. We then asked whether the reduction of Rca-α: impaired light-dependent regulation of Rubisco activity, enhanced the photosynthesis and/or growth of soybean, or altered total Rubisco content or the thermotolerance of photosynthesis.

Methods and materials

Plant transformation

The primers 5′-ATGGCAAAGCAGCTCAGCAAGT-3′ and 5′-GGATAACAATCCAATATGAACAAG-3′ were used to clone a 202 bp portion of the C-terminal extension and 3′-UTR of the Glyma02g249600 mRNA into both insertion sites of the pB7GWIWG2(II) GATEWAY™ destination vector (Karimi et al. 2002). The identity and proper orientation of the inserted sequences was verified with Sanger sequencing, which also revealed that one of the insertion sites contained additional DNA corresponding to various GATEWAY vectors. The full length and sequence of this additionally inserted DNA was not determined. Constructs were transformed into Agrobacterium strain EHA101 for soybean transformation at the ISU Plant Transformation Facility. The Williams 82 cultivar was transformed by organogenesis as previously described (Paz et al. 2006; Paz and Wang 2009) to generate 20 unique transformation events. Samples from all 20 lines were screened via Western blot, six of the lines were found to contain no visible Rca-α protein, and these lines (designated 77–6, 77–32, 78–13, 78–18, 78–34, and 78–39) were selfed to produce segregating T2 plants. Western blotting was used to test for the presence of Rca-α in each generation. To control for epigenetic changes that may have been introduced by the transformation procedure, plants lacking Rca-α expression (-Rca-α) were compared to transgenics that had regained Rca-α expression (+Rca-α) during segregation (i.e. azygous controls).

Growth conditions

Chamber-grown plants were grown in 21 cm (dia) × 21 cm (h) pots under a 16 h photoperiod at 26 °C and 60% RH. The light level at the top of the pots was approximately 300 µmol m^{-2} s^{-1} PPFD.

Field-grown plants were grown on a plot at the Energy Farm at the University of Illinois Urbana-Champaign (www.energyfarm.illinois.edu) during the summer of 2019. The plot was prepared as previously described (Kromdijk et al. 2016) and was rain fed. Plots ~ 3 m × 5.5 m and contained 6 separate experimental rows bordered by a single layer of wild type Williams 82. There were 30 inches between each row and between rows and the border. Each row contained 36 plants spaced 1.5 inches apart. Two rows were planted for each of the 3 independent lines (77–32, 78–13, and 78–39) tested, one containing seeds from azygous plants that had lost the RNAi phenotype during segregation, and one containing seeds from plants that had retained the phenotype. Seeds were planted on June 6th and harvested on October 10th. Measurements were made between July 28th and August 4th. A closed canopy had not formed at the time of measurements. The eastern edge of the Williams 82 border, as well as a few plants in the adjacent experimental row, were largely destroyed by rabbits in late June and early July, prior to the application of capsaicin powder, at which point the damage stopped (Fig. S1). Japanese beetles also caused significant damage to the 1st and 2nd trifoliate leaves during late June and early July, before being controlled by an application of pesticide.

Growth analysis

During growth chamber experiments, the length of the middle leaflet of the second trifoliate leaf was measured daily during the first half of the photoperiod. R (R Core Team 2018) and R-Studio (RStudio Team 2016) were used to fit the leaf elongation data to the sigmoidal formula:

$$Y = Y_0 + \frac{E}{1 + e^{(X_0 - X)/S}} \quad (1)$$

where Y corresponds to the leaf length and X corresponds to the number of days since sowing (Cookson et al. 2005, 2007). The fitted parameters include X_0 as the time of the curve inflection, Y_0 as the initial leaf length after emergence, E as the total amount of leaf expansion, and S as the slope parameter. $Y_0 + E$ is equal to the final length achieved by a leaf. From the fitted sigmoidal curves, the maximal leaf elongation rate (LER_{max}) was calculated as the slope at the point of inflection by the formula:

$$\mathrm{LER}_{\max} = \frac{E}{4S} \tag{2}$$

Specific leaf area was measured from the third leaflet of trifoliate leaves used for gas exchange. Leaflet photographs were analyzed using Easy Leaf Area (Easlon and Bloom 2014). Leaflets were dried for 3 days at 55 °C before measuring dry weight. Internode lengths and above ground dry weight of chamber grown plants were measured 12 weeks after sowing. Biomass of field grown plants was determined after plants had fully senesced. Shoots were dried for 2–3 weeks before biomass measurements.

SDS-PAGE and western blotting

The abundance of Rca-α, Rca-ß and Rubisco were measured with western blots. Leaf total protein was extracted by grinding tissue in buffer containing 62.5 mM Tris–HCl, pH 8.0, 2% SDS, 1 M urea, 10% glycerol, 5% 2-mercaptoethanol and 0.005% bromophenol blue. Electrophoresis was performed at 60 V through the (2.5% acrylamide) stacking gel and 140 V through the (10% acrylamide) running gel. Running buffer contained 25 mM Tris, 192 mM glycine, and 0.1% SDS. Proteins were transferred at 200 mA for 2 h onto Immobilon-FL PVDF membrane (MilliporeSigma, Burlington, MA, USA) in buffer containing 25 mM Tris, 192 mM glycine and 0.05% SDS. All subsequent steps were performed at room temperature. Blocking was in phosphate buffered saline (PBS) containing 5% cold water fish gelatin (G7765, Sigma) for 1 h. Membranes were incubated overnight in PBS with Tween 20 (PBST) containing an anti-Rca antibody diluted 1:4000. The Rca antibody was a custom, polyclonal antibody produced by GenScript (Piscataway, NJ, USA) against the peptide antigen CELESGNAGEPAKLIR. This sequence is highly conserved among Rca homologs. Secondary incubation of membranes was for 1 h in PBST containing Goat anti-Rabbit IgG conjugated to Alexa Fluor® 680 (Cat. # A-21109, Thermo Fisher Scientific, Waltham, MA, USA) diluted 1:20,000. Membranes were scanned, and densitometry performed, using an Odyssey® CLx Infrared Imaging System (LI-COR Biosciences, Lincoln, NE, USA). After imaging the antibody bands, total protein and Rubisco was visualized by staining the PVDF membrane with Coomassie brilliant blue G-250. The recombinant *Arabidopsis* Rca-ß used to quantitatively assess the leaf endogenous levels of Rca-ß was produced as previously described (Kim et al. 2019).

Photosynthesis measurements

Gas exchange measurements were made on the youngest fully expanded trifoliates of seven- to eight-week-old plants. In the chamber experiments this corresponded to the third trifoliate leaf, while in the field it corresponded to a much later trifoliate. Measurements were made using LI-COR 6400 s equipped with Leaf Chamber Fluorometer heads (LI-COR p/n 6400-40). Instruments were warmed up for at least one hour prior to the beginning of measurements. CO_2 was provided at 400 µmol mol^{-1} (except during measurement of CO_2 response curves), and temperature was controlled at the level of the block.

Light response curves were first made at 26 °C to determine the proper light level for induction measurements. Leaves were dark adapted for 30 min in the chamber, after which gas exchange and fluorescence were measured at 5 min intervals at 0, 15, 30, 50, 75, 110, 150, 200, 275, 375, 500, 650, 800, 1000, and 1500 µmol m^{-2} s^{-1} PPFD. CO_2 assimilation (A), absorbed light ($PPFD_{abs}$), and day respiration (R_d, estimated as the linear intercept of the low light data points) were fit to:

$$A = \frac{\mathrm{PPFD}_{\mathrm{abs}} * A_{\max}}{\mathrm{PPFD}_{\mathrm{abs}} + I_{50}} - R_{\mathrm{d}} \tag{3}$$

The estimated constants were A_{max}, the maximum potential assimilation rate at infinite light, and I_{50}, the light level at which assimilation is half of A_{max} (Lobo et al. 2013).

Photosynthesis induction assays consisted of 10 min of darkness, followed by 20 min of low light, followed by 45 min of high light. Low/high light was 20/500 and 100/1700 µmol m^{-2} s^{-1} PPFD during growth chamber and field experiments, respectively. Experiments were conducted at 26 °C and 38 °C for chamber-grown plants, and at 28 °C for field-grown plants. For the 38 °C experiments, plants were kept at 38 °C for 2 h in darkness prior to beginning the previously mentioned PPFD regime. The contribution of stomatal opening to induction was removed by normalizing the assimilation rate to a standard internal CO_2 concentration of 250 µmol mol^{-1} ($C_{i,f}$). The normalized assimilation rate, A^*, was calculated as $(A + R_d)(c_{i,f}/c_i)$ (Taylor and Long 2017), where R_d for each curve was taken as the gross assimilation during the dark adaptation period. Through log-transformation and linear regression, A^*, the normalized assimilation rate at time t, and A^*_f, the normalized assimilation rate at the end of induction, were fit to the formula:

$$A^* = A^*_{\mathrm{f}} - (A^*_{\mathrm{f}} - A_{\mathrm{i}})\mathrm{e}^{-t/\tau_{\mathrm{s}}} \tag{4}$$

–as previously described (Woodrow and Mott 1989; Hammond et al. 1998). The region used in fitting varied slightly between curves but most often contained the data from 2 to 7 min after the light transition. The estimated constants were τ_s, the photosynthetic induction rate constant, and A_i, the CO_2 fixation capacity of Rubisco at the beginning of induction.

CO_2 response curves were measured after induction on the same leaf section. The sequence of CO_2 concentrations

(μmol mol^{-1}) was 400, 350, 300, 200, 100, 50, 400, 450, 500, 600, 800, 1000, 1500, and 400 at 3 min intervals in the chamber experiments and 400, 200, 100, 50, 400, 600, 800, 1200, 2000 at 2.5 min intervals in the field experiments. Curves were fit for V_{cmax}, J_{max}, and R_d, on the basis of C_i, using the default method in the 'plantecophys' package for R (Duursma 2015). Induction and CO_2 response curves at 26 °C were measured prior to and on adjacent leaflets to curves measured at 38 °C.

Leaf absorbance measurements were based on the external method (Olascoaga et al. 2016), and were made using a JAZ spectrometer equipped with a SpectroClip Probe (Ocean Optics, Largo, FL, USA), on an unused leaflet from all trifoliates used in gas exchange. The cumulative absorbance in the Leaf Chamber Fluorometer head, which contains red and blue LEDs, was calculated from the corresponding red and blue wavelengths using a custom R script.

Rubisco activation state

High light samples were collected at the end of the CO_2 response curves and thus are also the leaf areas on which induction was measured. Low light adapted samples were obtained from another portion of the same leaflet. Samples were immediately frozen in liquid nitrogen and stored at − 80 °C until used in assays. Rubisco catalytic sites were measured by the binding of radiolabeled carboxypentitol-1,5-bisphosphate (^{14}C-CPBP, 1.23×10^5 DPM $nmol^{-1}$), which was prepared from K^{14}CN as described in Kubien et al. 2011. Modifications for the determination of in vivo activation were as previously described (Butz and Sharkey 1989; Choquette et al. 2020). Briefly, upon assaying, samples were ground with a tenbroeck glass tissue homogenizer in N_2-sparged CO_2-free extraction buffer (50 mM EPPS-NaOH pH 8, 1 mM EDTA, 5 mM MgCl2, 1% PVPP, 5 mM DTT, and 1% protease inhibitor cocktail (Sigma-Aldrich P9599); pH 8.05) and pelleted for 30 s. For measurement of initial Rubisco active sites, sample extracts were incubated on ice with 20 μM ^{14}C-CPBP for 30 min. Then, 1.5 mM ^{12}C-CPBP and 100 μL of activation buffer (50 mM EPPS-NaOH pH 8, 1 mMEDTA, 20 mM $MgCl_2$, 30 mM $NaHCO_3$) were added and incubated at room temperature for 20 min. For measurement of total Rubisco active sites, sample extracts were incubated for 20 min at room temperature with an equal volume of activation buffer, then incubated with 3 mM ^{14}C-CPBP for 30 min at room temperature. Following incubation, unbound ^{14}C-CPBP was separated from Rubisco by passing samples through 0.7×30 cm chromatography columns packed with Sephadex G-50. Radioactivity in the column fractions was quantified with a liquid scintillation counter (Packard Tri-Carb 1900 TR, Canberra Packard Instruments Co., Downers Grove, IL). Leaf extract supernatants were frozen and their protein content was measured by Bradford assay at a later date.

Statistical analysis and independent lines

Unless otherwise stated, statistical tests were by type II ANOVAs calculated using the 'Anova' function in R's 'car' package. Each plant measured was treated as an individual biological replicate. Growth chamber experiments used three independent lines. Each line contributed at least one plant to the -Rca-α group and at least one plant to the control group. Due to seed limitations, as well as inter-generational loss of the RNAi phenotype, the field study was drawn from only a single line of the three independent lines used in the growth chamber studies.

Results

Reduction of Rca-α content did not alter Rubisco or Rca-ß content

A search of Soybase indicated that 5 loci are predicted to encode isoforms of Rca in soybean: Glyma02g249600 and Glyma14g067000 for isoforms of Rca-α, Glyma18g036400 and Glyma11g221000 encode for isoforms of Rca-ß, and Glyma03g068100 (through differential splicing) for both Rca-α and Rca-ß (Fig. 1A). It also indicated that, in non-stressed leaves, the two Rca-α encoding loci produce equal amounts of transcript, as do the two Rca-ß encoding loci, while Glyma03g068100 is essentially non-expressed. To reduce Rca-α contents specifically, RNAi constructs were targeted against a region of mRNA that was highly conserved in both Rca-α encoding genes but poorly conserved in the others (Fig. 1B). Transformation of Williams 82 with these constructs reduced the leaf content of Rca-α protein while having no discernible impact on Rca-ß protein (Fig. 2). The Rca-α band (normally ~ 10% as intense as Rca-ß in wild type), was rendered invisible to the naked eye, and thus too faint for the degree of reduction to be accurately measured via Western blotting. To ensure that Rca-ß protein did not increase to compensate for the reduction of Rca-α, the Rca-ß content of field-grown plants was determined by quantitative Western blotting. Samples for this analysis were collected from leaflets used in gas-exchange following the conclusion of those measurements. Preliminary experiments indicated that our protocol for Western blot sampling resulted in approximately 40 ng of Rca-ß protein being loaded into each lane. A dilution series of purified *Arabidopsis* recombinant Rca-ß protein confirmed that this amount of Rca protein fell within the linear range of the sensitivity of our Rca antibody (Fig. S2A). Subsequent quantifying gels for Western blot analysis were loaded with a single lane of recombinant

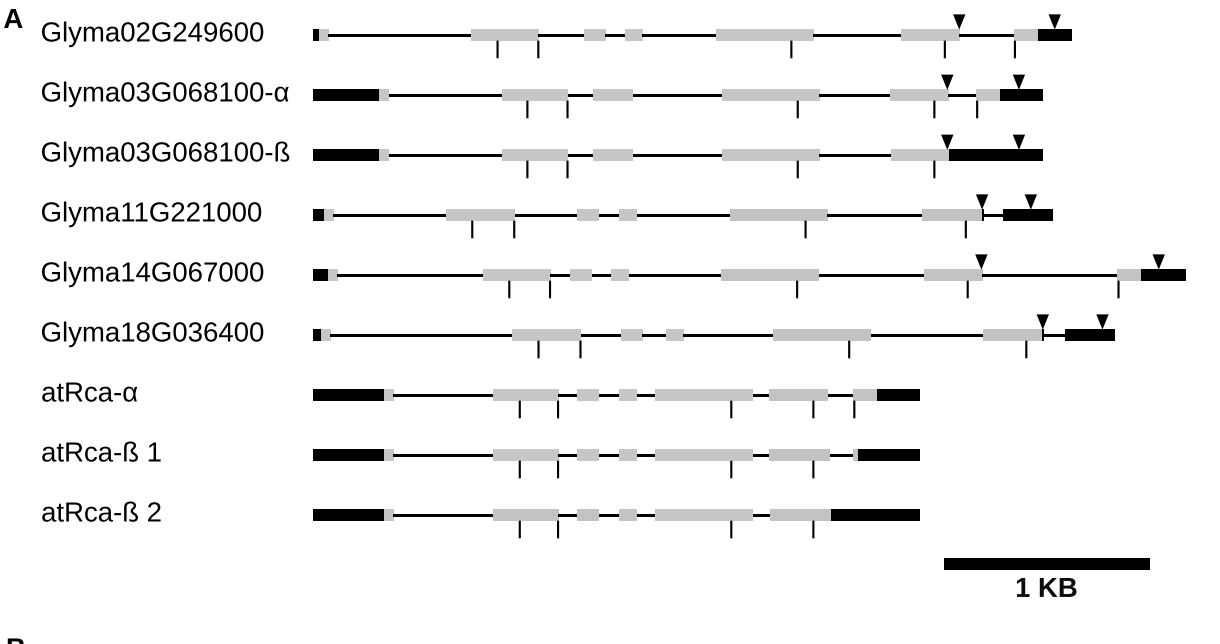

B

```
Glyma02G249600 ATGGCAAAGC AGCTCAGCAA GTAAACATTC CCGTTCCTGA AG---GTTGT ACTGATCCAA ATGCCTCAAA CTTCGACCCA
Glyma03G068100    GAC    G          TC TG      T  C                C       C  T  C   TGA      AT  T
Glyma11G221000  G CA  GCA  A  TG           T   T  T                  G          G   T-----  ----------
Glyma14G067000    .          C             A
Glyma18G036400  G CA  GCA  A  TG           T   T  T    G       GTT          A        G   T-----  ----------

Glyma02G249600 ACTGCAAGAA GTGATGATGG AACCTGCTTA TACACACCCT GAGAACCTAA GCATTCTCCA CTTGGAGAGA AGCTA-----
Glyma03G068100   A  C           G    AC       A TTT  AG ----  G  TTC  AGGT  AA T T   T   A  AATAT
Glyma11G221000 ------          TG          T   G G   ACATT T  AGA TT  C  A G CT AGG TGCAA    G   A GC   C
Glyma14G067000                                                                    A
Glyma18G036400 ------          TG          T   G G   ACATT T  AGC TT  C  ATG CT AGG TGCAA        A GC   T

Glyma02G249600 AGAGTTGAGA TAATAAAATA A--------- GTTATCTTGT TCATATTGGA TTGTTATCC
Glyma03G068100   TT     A  C GC        AAGAATGTT ACA  G  T  C  C   A   A TCAC TT
Glyma11G221000  AGT        G  TTT -- -           -C   A  T              C   CT
Glyma14G067000 T  C           C                 T
Glyma18G036400  AGT         G  CTT -- -          -C   A  T              CC  CT
```

Fig. 1 **A** Gene structural overview of soybean and *Arabidopsis* genes that encode for Rca. Thick horizontal black and grey bars indicate untranslated and protein coding portions of the mature mRNA, respectively. Thin horizontal lines indicate introns. Vertical lines mark (in order) the following corresponding regions of the protein product: chloroplast targeting peptide, N-domain, α/ß domain, α-helical domain, C-domain, and C-terminal extension. Models with only 4 vertical lines do not encode a C-terminal extension. The inverted triangles indicate the region of sequence targeted by the RNAi construct. **B** mRNA sequence alignment showing RNAi-targeted regions of soybean Rcas. The cloned portion of the Glyma02g249600 mRNA used in RNAi vector construction is shown in the top line consensus sequence; the binding sites of the cloning primers are underlined. Exon junctions are indicated by the dots at positions 2 or 3. Conserved residues are omitted from non-consensus sequences

Rca-ß protein, 7 sample lanes, a molecular weight ladder, and a single lane of wild type protein. The gel-to-gel variation was large (Fig. S2B), with the coefficient of variation of the wild type samples being 0.98. Normalizing the intensity of each gel using the lane of recombinant Rca-ß protein (Fig. S2C) reduced the coefficient of variation of the wild type samples to 0.54. Averaging all lanes from all of the gels revealed no significant difference in the content of Rca-ß between the + Rca-α, -Rca-α, and wild type samples (Fig. S2D).

Determination of Rubisco content from ^{14}C-CPBP binding (Table S1) showed that field grown plants contained, on a leaf area basis, four times more Rubisco than chamber grown plants, but no significant effect from the presence of Rca-α. The soluble protein contents of growth chamber grown + Rca-α and -Rca-α plants were determined by Bradford assays to be 7.6 ± 0.9 g m^{-2} and 7.3 ± 0.7 g m^{-2}, respectively.

An inducible or post-translationally modified Rca accumulated in field-grown soybean

Samples were collected from the third and fourth trifoliates of field-grown plants in early July to assay for the presence of Rca-α. It was discovered that only one of the three transgenic lines that had been planted still displayed the RNAi phenotype. In addition, ~ 30% of the leaf samples contained evidence of novel or post-translationally modified Rca (Fig. S3). These isoforms occurred at molecular weights ~ 1kD larger than Rca-α and Rca-ß, and their abundance appeared in many cases to be inversely correlated with the abundance of the constitutive isoforms. Unfortunately,

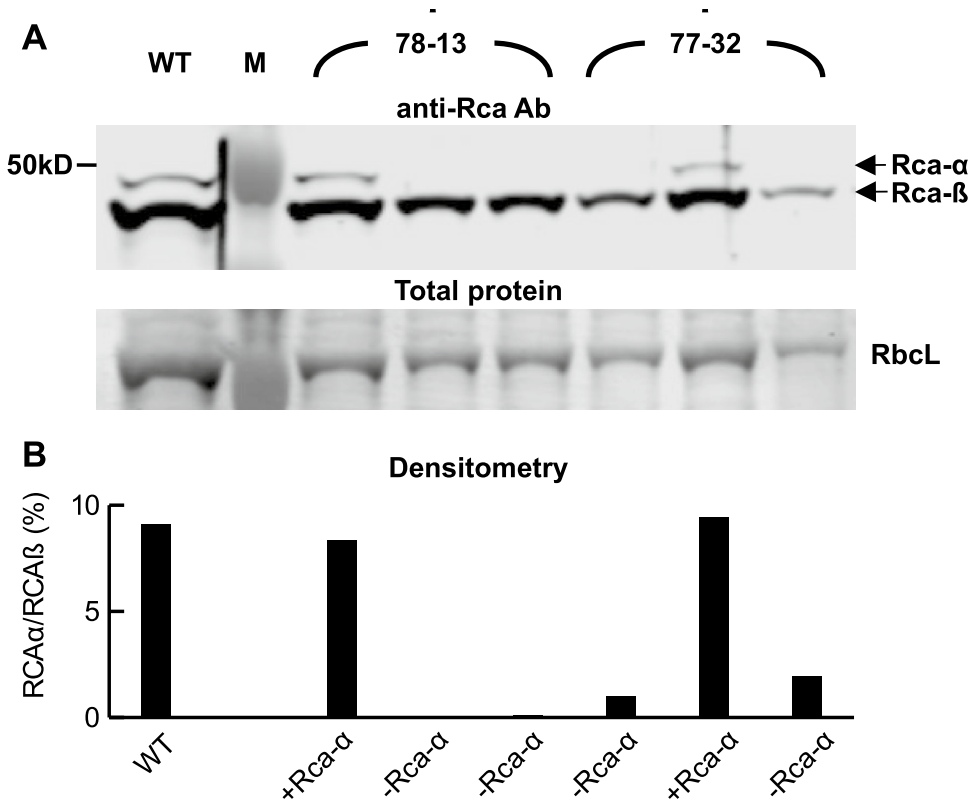

Fig. 2 Western blot (**A**) and densitometry (**B**) based determination of Rca-α presence of wild-type (lane 1) and transgenic (lanes 3–8) soybean. M contains the ladder. Percentages in **B** were determined by dividing the intensity of the Rca-α band by the intensity of the Rca-ß band. The determined Rca-α status of each of the segregating transgenics is shown at the bottom of **B**

the proximity of the novel Rca-ß band to the constitutive Rca-α band made it difficult to unequivocally determine the Rca-α status of samples whose bands were not clearly resolved. In follow-up samples collected in mid July from these same leaflets, only ~ 10% of the samples showed evidence of the novel isoforms, indicating that they were transient. None of the samples collected on August 14th from the leaves previously used in gas exchange contained these novel isoforms. We speculate that these Rcas may have been induced by stress, either from the previously mentioned herbivory damage to the 1st and 2nd trifoliate leaves, or from heat and were not explored further.

Reduction of Rca-α content did not affect photosynthesis or growth

During the growth chamber studies, appropriate light levels were determined from light response curves performed prior to induction and CO_2 response curves. The + Rca-α and -Rca-α transgenics responded identically in these experiments (Table S2). 500 µmol m^{-2} s^{-1} PPFD achieved ~ 90% of the maximum assimilation observed at 1500 µmol m^{-2} s^{-1} PPFD, and was selected as the light level for the subsequent response curves.

Photosynthetic induction curves of -Rca-α and + Rca-α plants were nearly identical (Fig. 3), and did not yield statistically significant differences in the fitted parameters τ_s, A_i, or A_f (Table S3). Photosynthetic induction tended to be slower during heat stress (Fig. 3B), though not quite significantly ($p = 0.07$). The field-grown plants took significantly longer to fully induce than the chamber-grown plants (Fig. 3C), though they also reached a significantly higher A_f by the end of induction. J_{max} and V_{cmax} were also not significantly impacted by the presence of Rca-α (Table S3). Temperature did have a significant impact on both parameters ($p < 0.05$), with 38 °C causing a decrease in V_{cmax} and an increase in J_{max}, relative to 26 °C.

The presence of Rca-α had an insignificant effect on all morphological parameters measured during the field experiment (Table S4), and an insignificant effect on all but one of the morphological parameters measured during the growth chamber experiments (Table S5). The maximal rate of elongation of the second trifoliate leaf occurred, for -Rca-α plants, 23.9 ± 0.3 days after sowing and, for + Rca-α plants, 25.0 ± 0.9 days after sowing. This result, though statistically significant by 2-way *t* test ($p = 0.03$), seems spurious, given the lack of impact of Rca-α on either photosynthesis or Rubisco biochemistry, and was most likely the result of variation in seedling germination during our assay.

Reduction of Rca-α content did not affect Rubisco activation

The Rubisco activation state of clamped sections of leaves was measured to correlate photosynthetic physiology to

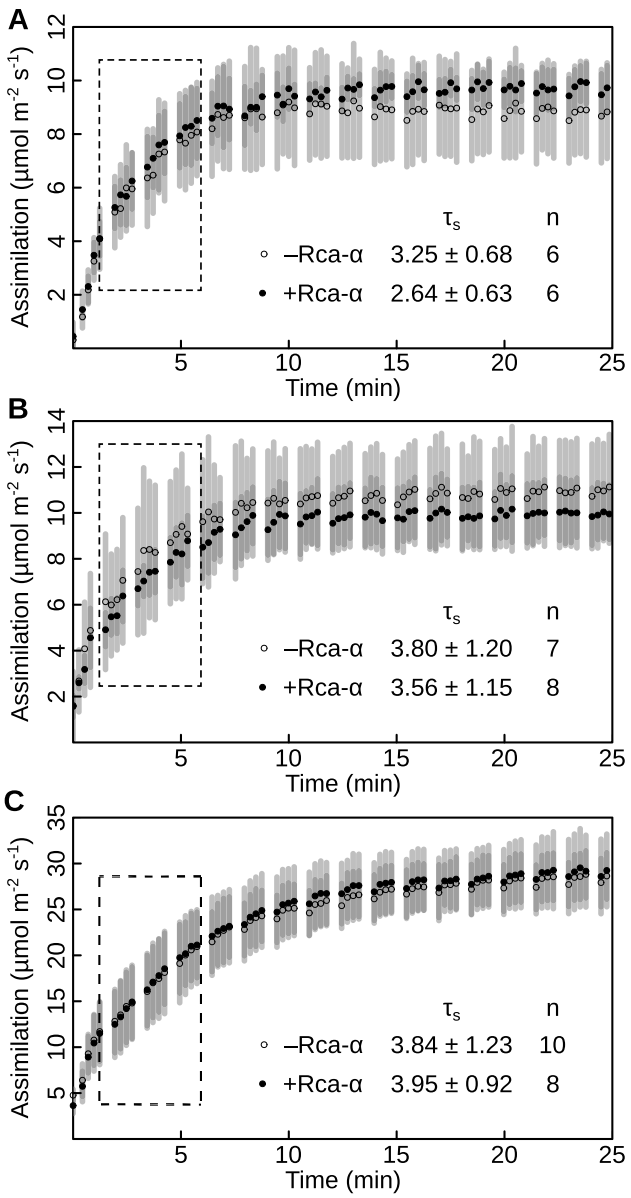

Fig. 3 Photosynthetic induction curves of transgenics in **A** growth chambers at 26 °C, **B** growth chambers at 38 °C, and **C** the field. A step increase of 20 to 500 μmol m^{-2} s^{-1} PPFD was used for the growth chamber measurements while a step increase of 100 to 1700 μmol m^{-2} s^{-1} PPFD was used for the field measurements. Error bars represent one standard deviation. Boxes indicate the portion of the response curve that was used for fitting the time constants (τ_s), which are inset in each graph along with the replicate numbers

the biochemical function of Rca (Table 1). As expected, light level had the strongest impact on Rubisco activation, with low light samples averaging 39% activation and high light samples averaging 60% activation. There was also a significant difference between our two growth locations. Rubisco from field-grown plants was, on average, activated 13 percentage points more under low light and activated 17 percentage points more under high light than Rubisco from chamber-grown plants. Twenty minutes after the start of induction the proportion of closed PSII reaction centers was 0.69 ± 0.08 and 0.60 ± 0.06 in the chamber and field experiments, respectively, indicating that the lower Rubisco activation of chamber-grown plants was not due to insufficient assay light levels. Rca-α had a nearly significant effect ($p = 0.08$), with the trend being towards higher activation in -Rca-α plants. This trend held in 4 of the 6 environment combinations that were tested, with the two strongest instances both occurring at high light and moderate temperature. No activation state greater than 76% was obtained for samples from fully light-adapted leaves, suggesting that the ^{14}C-CPBP/^{12}C-CPBP exchange protocol underestimated the *in vivo* Rubisco activation state.

Discussion

Stability of the RNAi phenotype and novel Rca isoforms

The stochastic nature of RNAi transgenes led to some difficulties during the course of the study. RNAi phenotypes may be lost from one generation only to re-emerge in subsequent generations (Zhong et al. 2013). This intergenerational instability precluded selfing the transformants for three-generations prior to characterizing them. It also necessitated that every plant on which measurements were conducted be pre-screened for the presence or absence of Rca-α. This requirement, along with the small number of generations, limited the amount of seed available for field studies. This was further exacerbated by the apparent loss of the RNAi phenotype in two of the three lines planted in the field (Fig. S3). In addition to its transgenerational instability, RNAi sometimes expresses in a patchy, rather than systemic, manner within individuals (Kunz et al. 1996). Due to this chimerism, and the fact that a different leaf section was sampled for Western Blotting than for the induction and Rubisco activity measurements, the Rca-α status of the two areas could differ. During the field study, a subset of plants had their Rca-α status tested at both their third trifoliate leaf and from the leaflet used in gas exchange measurements. Out of 23 total comparisons, there was only a single instance where the Rca-α status of the two sampled areas differed. This suggests that chimerism in our lines was not significant enough to affect our overall conclusions.

It is unclear whether the novel Rca isoforms observed during the field study were the result of a post-translational modification of the existing Rca, or due to the expression of an inducible isoform. The inverse correlation of their presence to the presence of the constitutive Rca isoforms is very similar to the situation observed in winter wheat where heat-stress caused a downregulation of the constitutive Rca

Table 1 Summary and ANOVA statistics of Rubisco activation state (%) determined from ^{14}CPBP binding

Location	Temp (°C)	Light	Rca-α	*N*	Mean	SD	*P* value
Growth chamber	26	Low	+	9	39	12	Location: 2.8×10^{-9}
			–	4	32	12	
		High	+	9	51	6	
			–	5	59	13	Temp: 0.54
	38	Low	+	8	32	4	
			–	4	36	8	
		High	+	8	55	6	Light: 2.2×10^{-16}
			–	4	52	4	
Field	28	Low	+	10	46	6	
			–	8	49	7	Rca-α: 0.08
		High	+	10	65	6	
			–	8	76	12	

isoform and upregulation of a more heat-stable version (Scafaro et al. 2019a; Degen et al. 2021). Further characterization of these novel isoforms is needed to determine their molecular nature and the environmental conditions that cause their formation.

Comparison of in vivo and in vitro measurements of Rubisco activity

The in vivo catalytic turnover rate of Rubisco, estimated by dividing V_{cmax} (Table S3) by leaf Rubisco content (Table S1) ranged from 13.2 to 9.7 s^{-1} in the chamber experiments to 7.5 s^{-1} in the field experiments, significantly higher than the in vitro turnover of soybean Rubisco, 4.1 s^{-1} (Orr et al. 2016). However, in vivo turnover estimates are routinely 1.2–1.3X higher than in vitro estimate (von Caemmerer 2000; Walker et al. 2013). Additionally, while the V_{cmax} of our field-grown soybean lies within previously reported ranges (Ainsworth et al. 2004; Betzelberger et al. 2012), the use of the Rubisco kinetic parameters of Bernacchi et al. (2002), as well as deactivation of Rubisco at low CO_2 in our AC_i curves, may have caused it to be systematically overestimated. The Rubisco kinetic parameters of Bernacchi et al. (2002) can over-estimate V_{cmax} of *Arabidopsis* by as much as 40% at high temperatures (Walker et al. 2013), and may do so similarly in soybean. Rubisco deactivation at low CO_2 may have been caused by the length of our AC_i step intervals, which, at 2.5 min and 3 min in the field and chamber experiments, respectively, were longer than the < 2 min that has been recommended (Long and Bernacchi 2003). The more reasonable turnover rate obtained from the field experiments supports this possibility.

The initial activity of Rubisco estimated from the induction curves by A_i/A_f (Table S3, ~ 15–20%) was consistently lower than the initial activity estimated from CPBP binding (Table 1, ~ 30%). Part of this difference may be caused by the presence of 2-carboxyarabinitol-1-phosphate (Ca1P) at low light. Ca1P, synthesized in darkness by a dedicated enzyme in some plants, including soybean, inhibits Rubisco prior to being degraded in the light. CABP binds Rubisco more tightly than Ca1P, effectively outcompeting and replacing it. Carbamylated, Ca1P-bound Rubisco is therefore unable to contribute to a leaf's carboxylation capacity, despite being scored as activated (Butz and Sharkey 1989).

The activation state of Rubisco never exceeded 80% (Table 1), even in fully illuminated leaves. Rubisco activation under similar conditions is frequently reported to exceed 85% (Crafts-Brandner and Salvucci 2000; Salvucci et al. 2006), suggesting that our assays underestimated activation. It is possible that this underestimation was the result of Rubisco deactivation during the initial protein extraction steps, which can occur when centrifugation is longer than even 30 s (Sharwood et al. 2016). It could also have been caused, in theory, by a greater degree of non-specific binding of CPBP in the "total" than "initial" assay mixtures. This seems unlikely, however, as the concentration of CPBP never exceeded 45 µM in our assays, at which level non-specific binding should account for less than 10% of the total bound counts (Yokota and Canvin 1985). After labeling, our assays also included a large excess of non-radiolabeled CPBP and a chromatographic purification step, both of which would have further reduced the effect of non-specific binding.

Rca-α does not enhance the thermal stability of photosynthesis in soybean

Rca denaturation is believed to be a major limitation to photosynthesis at elevated temperature (Crafts-Brandner and Salvucci 2000). Although Rca-α is more thermally stable than its conjugate Rca-ß (Keown and Pearce 2014), the results of this study suggest that the C-terminal extension of soybean Rca-α does not enhance protein thermal stability (Table S3). This is more consistent with the situation in rice (Shivhare and Mueller-Cajar 2017; Shivhare et al.

2019), agave (Shivhare and Mueller-Cajar 2017), and wheat (Scafaro et al. 2019a; Degen et al. 2020), where differences in isoform thermal stability appear to be the result of amino acid substitutions within the N-domain and AAA + core domains (Fig. S4). The same is likely true in *Arabidopsis*, as the assimilation of wild-type and Rca-α or Rca-ß expressing mutants responded similarly to increasing temperature (Kim and Portis 2005; Salvucci et al. 2006). In Salvucci et al. (2006), PSII fluorescence increased starting at 35 °C in *Arabidopsis* with reduced total Rca, while an Rca-ß expressing mutant and wild type did not display any increase up to 45 °C, suggesting that the amount of Rca has a greater impact on photosynthetic thermotolerance than does the composition of isoforms. Our data is consistent with this interpretation.

The Rca-encoding loci of soybean are largely invariant at amino acid positions that have been previously implicated in thermostability. The majority of these positions are located within the AAA + domain, which is composed of an α-ß and an α-helical subdomain (Fig. S4). Mutations in this region affect Rca thermal stability either by altering the packing of the hydrophobic core or by altering interactions between the α-ß and α-helical subdomains of adjacent Rca monomers: interactions that drive Rca oligomerization (Stotz et al. 2011). An N99-R294 pair in tobacco, which forms a thermostabilizing hydrogen bond between adjacent monomers (Keown and Pearce 2014), is present in each soybean Rca isoform (Fig. S4). Furthermore, in wheat Rca, an M159I mutation increased the thermal optimum of ATPase activity by ~ 5 °C (Degen et al. 2020). Soybean Rca-α is encoded by both a methionine (Glyma02g249600) and an isoleucine (Glyma14g067000) containing locus, whose expression levels are roughly equal. The same is true for the two Rca-ß encoding loci. Reduction of leaf Rca-α content would therefore not be expected to alter the M to I ratio at this position, or consequently, the thermal stability of Rca. Finally, soybean Rca loci are predominantly invariant at 10 other positions (Fig. S4, alignment positions 63, 77, 269, 274, 281, 311, 338, 363, 365, and 367) implicated in the thermal stability of wheat Rca (Scafaro et al. 2019a). Taken as a whole, the amino acid identities of Rca-α and Rca-ß are consistent with the two isoforms having similar thermal profiles.

The soybean Rca-ß C-Domain contains features that confer ADP sensitivity

That reduction of soybean Rca-α contents does not impair Rubisco deactivation in low light suggests that soybean Rca-ß could be more sensitive to ADP inhibition than its homolog in *Arabidopsis*. This is true in tobacco, which does not express any Rca-α (Carmo-Silva and Salvucci 2013). Carmo-Silva and Salvucci (2013) showed that the ADP sensitivity of tobacco Rca-ß could be eliminated by mutating 17 amino acids within the two AAA + subdomains and the C-Domain (Fig. S4, starred positions) to the corresponding amino acids in *Arabidopsis*. Overall, soybean Rca-ß has a similar degree of conservation to *Arabidopsis* and tobacco Rca-ßs at these 17 positions, but is more similar to *Arabidopsis* at the AAA + domain sites, and more similar to tobacco at the C-Domain sites. The C-Domain is close to the nucleotide binding pocket of adjacent subunits and contains a critical tyrosine (Fig. S4, position 364) that is essential for ATPase and activase activity (Stotz et al. 2011). In wheat Rca, mutating two position, T358K and Q362E, was sufficient to confer ADP sensitivity (Perdomo et al. 2019). Soybean Rcas contain K and E at these two positions. Two mutations of wheat Rca-α, K381R and K381Q, led to increased and decreased maximal ATP hydrolysis, respectively, which was mediated through modulation of the mutants' affinity for ATP rather than their affinity for ADP (Scafaro et al. 2019b). The authors concluded that the presence of a basic amino acid at this position enhanced interaction with the γ-phosphate of ATP, which in turn enhanced ATP binding and decreased ADP sensitivity. This result supports the view that soybean Rca-ß is natively ADP sensitivity, as both Rca-ß encoding loci contain non-basic serine residues at this position.

A low Rca-α/Rca-ß ratio is likely an indicator of self-regulating Rca-ß isoforms

It has been previously suggested that Rca-ß produced from differentially spliced loci that produce both α and ß are insensitive to ADP inhibition, while Rca-ß produced from non-differentially spliced loci are sensitive (Perdomo et al. 2019). The results of the present study support that generalization. We propose that another simple indicator of the regulatory properties of Rca-ß may be the relative abundance of Rca-α and Rca-ß. While the composition of Rca isoforms of most species has yet to be determined, it is possible that several other crops that express a similarly low abundance of Rca-α, such as wheat (12% α) (Perdomo et al. 2019; Degen et al. 2021), rice (10–20% α) (Zhang and Komatsu 2000), spinach (10–20% α) (Werneke et al. 1989) and barley (33% α) (Rundle and Zielinski 1991), will not benefit tremendously from its removal.

Why does soybean Rca-α exist?

The redox status of the C-terminal extension appears to modulate the affinity for ATP (Scafaro et al. 2019b), which in turn alters the perceived sensitivity to ADP inhibition. This redox input may be of secondary physiological utility, given that control by stromal ATP/ADP alone is sufficient for tobacco and, by the results of this study, soybean. The supply

of ATP equivalents is likely more susceptible to disruption than the supply of reducing equivalents, as the ATP:NADPH ratio produced by linear electron transport is lower than that required by the Calvin-Benson-Bassham cycle, and requires the ATP deficit to be made up by cyclic electron transport (Sharkey and Zhang 2010; Foyer et al. 2012).

It seems likely that the benefit conferred by Rca-α, and therefore the selective pressure to maintain it, are dependent on the prevailing growth conditions of a plant, and that its presence is adaptive in environments where large changes in the redox status of the stroma occur even during periods of illumination. One such condition might be an abundance of rapid but transient heat stress events, as stromal oxidation occurs, alongside a decrease in the ATP/ADP ratio, within seconds following the rapid heating of illuminated tobacco from 30 to 40 °C (Schrader et al. 2007). Under such circumstances, in addition to being more thermo-stable (Keown and Pearce 2014; Zhang et al. 2015), being sensitive to the stromal redox status could allow Rca to modulate its activity more rapidly or to a greater extent than would be allowed by ATP/ADP sensitivity alone. Redox sensitivity could also become more important under various other stress conditions where increased demands are placed upon the supply of NADPH. NADPH oxidases, for example, draw directly from the pool of reducing equivalents to supply reactive oxygen species that function as stress signaling compounds (Foyer and Noctor 2012) (Table 2).

Although there is no direct evidence for it currently, the C-terminal extension of Rca-α might also bind ancillary proteins. Such interactions would probably be quite weak, but this does not mean that they could not produce biologically significant effects on signaling or metabolic pathways (Sukenik et al. 2017), especially when one considers the relative abundance of Rca compared to traditional signaling components. Such a role for Rca has been suggested previously, as *Arabidopsis* expressing a T78S Rca-ß site-directed mutant had a large number of gene-expression changes relative to wildtype *Arabidopsis*

Table 2 Summary and ANOVA statistics of photosynthetic parameters estimated from induction and CO_2 response curves

	Location	Temp (°C)	Rca-α	*N*	Mean	SD	*P* value
τ_s (min)	Growth Chamber	26	+	6	2.6	0.6	Location:
			–	6	3.3	0.7	0.02
		38	+	8	3.6	1.1	Temp:
			–	7	3.8	1.2	0.07
	Field	28	+	8	4.0	0.9	Rca-α:
			–	10	3.8	1.2	0.52
A_i ($\mu mol\ m^{-2}\ s^{-1}$)	Growth Chamber	26	+	6	1.5	1.3	Location:
			–	6	1.4	1.1	0.002
		38	+	8	1.9	1.5	Temp:
			–	7	3.1	2.5	0.50
	Field	28	+	8	5.7	7.0	Rca-α:
			–	10	5.8	4.0	0.70
A_f ($\mu mol\ m^{-2}\ s^{-1}$)	Growth Chamber	26	+	6	10.1	4.0	Location:
			–	6	9.4	3.8	2×10^{-16}
		38	+	8	10.3	1.4	Temp:
			–	7	11.3	2.2	0.28
	Field	28	+	8	28.8	4.2	Rca-α:
			–	10	29.9	2.3	0.39
J_{max} ($\mu mol\ m^{-2}\ s^{-1}$)	Growth Chamber	26	+	8	98	11	Location:
			–	6	86	14	1.46×10^{-15}
		38	+	6	128	22	Temp:
			–	6	126	35	0.015
	Field	28	+	8	235	55	Rca-α:
			–	10	248	41	0.93
V_{cmax} ($\mu mol\ m^{-2}\ s^{-1}$)	Growth Chamber	26	+	8	55	6	Location:
			–	6	49	7	2.2×10^{-16}
		38	+	6	35	5	Temp:
			–	6	40	8	0.001
	Field	28	+	8	128	20	Rca-α:
			–	10	129	10	0.90

(Kim et al. 2019), despite the mutation having no effect on the rate of Rubisco activation *in vitro*. In hexameric Rca assemblies, the C-terminal extension is located opposite to the face that binds Rubisco, so interaction of it with ancillary proteins can occur concurrently with Rubisco interaction. In cyanobacteria, for example, a C-terminal "SSUL" domain that also contains a redox-sensitive cysteine pair was recently discovered to bind and recruit Rubisco to carboxysomes (Flecken et al. 2020).

Conclusions

Here, we report findings from transgenic soybean containing no immunologically detectable Rca-α, which we predicted based on previous *Arabidopsis* results would have higher photosynthesis and growth under fluctuating light. Instead we found that photosynthetic induction, photosynthetic thermal sensitivity, and growth were not enhanced under growth chamber and field conditions. The reduction of soybean Rca-α contents also did not enhance Rubisco activity in low light as was seen in *Arabidopsis*. Taken together, these results highlight the potential for differences in Rca isoform function among species, as well as the importance of validating crop improvement strategies in production species.

Given that studies of the in vivo function of Rca-α suggesting it as a potential target for manipulation to increase photosynthetic efficiency have been done in *Arabidopsis*, we felt it important to study the function of Rca-α in a crop. We used an RNAi construct targeted against the C-terminal extension to reduce the endogenous expression of Rca-α in soybean. In contrast to *Arabidopsis*, these soybean maintained the ability to regulate Rubisco activity in darkness and low light, did not have a significantly altered rate of photosynthetic induction, and achieved similar growth rates. This suggests a fundamental difference in the mechanism by which *Arabidopsis* and soybean regulate Rca activity. This difference is likely hinted at by the ratio of Rca-α to Rca-ß in these two species, as soybean contains only ~ 10% of its total Rca in the alpha isoform, while *Arabidopsis* contains a 1:1 α/ß ratio. The distinction may be driven by the different light environments that the two species are adapted to; *Arabidopsis* grows well even under low light conditions, while soybean is grown under full sunlight. Overall, our results emphasize the importance of validating crop improvement strategies not just in *Arabidopsis*, but also in production crop species. Biochemical characterization of the Rca isoforms in soybean is needed to better understand the enzymatic basis of their distinct physiological properties.

Supplementary Information The online version contains supplementary material available at https://doi.org/10.1007/s11120-022-00962-3.

Acknowledgements The authors would like to thank David W. Drag and Taylor L. Pederson for help with the field study and the reviewers for helping improve the manuscript.

Author contributions CMH wrote the manuscript and performed experiments. APC, SYK, KSS and RGE performed assays. DAW produced and maintained the primary transformants. JAP helped establish the Rubisco activation assay. DRO, CJB, MHS and SCH supervised the experiments and conceived the original research plans.

Funding This research was supported by the USDA National Institute of Food and Agriculture Grant 2015-67013-22835.

References

Ainsworth EA, Rogers A, Nelson R, Long SP (2004) Testing the "source–sink" hypothesis of down-regulation of photosynthesis in elevated [CO_2] in the field with single gene substitutions in *Glycine max*. Agric for Meteorol 122:85–94

Bernacchi CJ, Portis AR, Nakano H, von Caemmerer S, Long SP (2002) Temperature response of mesophyll conductance. Implications for the determination of Rubisco enzyme kinetics and for limitations to photosynthesis *in vivo*. Plant Physiol 130:1992–1998

Betzelberger AM, Yendrek CR, Sun J, Leisner CP, Nelson RL, Ort DR, Ainsworth EA (2012) Ozone exposure response for U.S. soybean cultivars: linear reductions in photosynthetic potential, biomass, and yield. Plant Physiol 160:1827–1839

Butz ND, Sharkey TD (1989) Activity ratios of Ribulose-1,5-bisphosphate carboxylase accurately reflect carbamylation ratios. Plant Physiol 89:735–739

Carmo-Silva AE, Salvucci ME (2012) The temperature response of CO_2 assimilation, photochemical activities and Rubisco activation in *Camelina sativa*, a potential bioenergy crop with limited capacity for acclimation to heat stress. Planta 236:1433–1445

Carmo-Silva AE, Salvucci ME (2013) The regulatory properties of Rubisco activase differ among species and affect photosynthetic induction during light transitions. Plant Physiol 161:1645–1655

Carmo-Silva AE, Gore MA, Andrade-Sanchez P, French AN, Hunsaker DJ, Salvucci ME (2012) Decreased CO_2 availability and inactivation of Rubisco limit photosynthesis in cotton plants under heat and drought stress in the field. Environ Exp Bot 83:1–11

Choquette NE, Ainsworth EA, Bezodis W, Cavanagh AP (2020) Ozone tolerant maize hybrids maintain Rubisco content and activity during long-term exposure in the field. Plant Cell Environ 43:3033–3047

Cookson SJ, Van Lijsebettens M, Granier C (2005) Correlation between leaf growth variables suggest intrinsic and early controls of leaf size in *Arabidopsis thaliana*. Plant Cell Environ 28:1355–1366

Cookson SJ, Chenu K, Granier C (2007) Day length affects the dynamics of leaf expansion and cellular development in *Arabidopsis thaliana* partially through floral transition timing. Ann Bot 99:703–711

Crafts-Brandner SJ, Salvucci ME (2000) Rubisco activase constrains the photosynthetic potential of leaves at high temperature and CO_2. Proc Natl Acad Sci 97:13430–13435

Degen GE, Worrall D, Carmo-Silva AE (2020) An isoleucine residue acts as a thermal and regulatory switch in wheat Rubisco activase. Plant J 103:742–751

Degen GE, Orr DJ, Carmo-Silva E (2021) Heat-induced changes in the abundance of wheat Rubisco activase isoforms. New Phytol 229:1298–1311

DeRidder BP, Shybut ME, Dyle MC, Kremling KAG, Shapiro MB (2012) Changes at the 3′-untranslated region stabilize Rubisco activase transcript levels during heat stress in *Arabidopsis*. Planta 236:463–476

Easlon HM, Bloom AJ (2014) Easy Leaf Area: automated digital image analysis for rapid and accurate measurement of leaf area. Appl Plant Sci. https://doi.org/10.3732/apps.1400033

Eckardt NA, Snyder GW, Portis AR Jr, Ogren WL (1997) Growth and photosynthesis under high and low irradiance of *Arabidopsis thaliana* antisense mutants with reduced Ribulose-1,5-bisphosphate carboxylase/oxygenase activase content. Plant Physiol 113:575–586

Flecken M, Wang H, Popilka L, Hartl FU, Bracher A, Hayer-Hartl M (2020) Dual functions of a rubisco activase in metabolic repair and recruitment to carboxysomes. Cell 183:457-473.e20

Foyer CH, Noctor G (2012) Managing the cellular redox hub in photosynthetic organisms: Cellular redox in photosynthetic organisms. Plant Cell Environ 35:199–201

Foyer CH, Neukermans J, Queval G, Noctor G, Harbinson J (2012) Photosynthetic control of electron transport and the regulation of gene expression. J Exp Bot 63:1637–1661

Fukayama H, Ueguchi C, Nishikawa K, Katoh N, Ishikawa C, Masumoto C, Hatanaka T, Misoo S (2012) Overexpression of Rubisco activase decreases the photosynthetic CO_2 assimilation rate by reducing Rubisco content in rice leaves. Plant Cell Physiol 53:976–986

Garcia-Molina A, Leister D (2020) Accelerated relaxation of photoprotection impairs biomass accumulation in Arabidopsis. Nat Plants 6:9–12

Hammond ET, Andrews TJ, Mott KA, Woodrow IE (1998) Regulation of Rubisco activation in antisense plants of tobacco containing reduced levels of Rubisco activase. Plant J 14:101–110

Hauser T, Popilka L, Hartl FU, Hayer-Hartl M (2015) Role of auxiliary proteins in Rubisco biogenesis and function. Nat Plants 1:1–11

Hayer-Hartl M (2017) From chaperonins to Rubisco assembly and metabolic repair. Protein Sci 26:2324–2333

He Z, von Caemmerer S, Hudson GS, Price GD, Badger MR, Andrews TJ (1997) Ribulose-1,5-bisphosphate carboxylase/oxygenase activase deficiency delays senescence of Ribulose-1,5-bisphosphate carboxylase/oxygenase but progressively impairs its catalysis during tobacco leaf development. Plant Physiol 115:1569–1580

Hutchison RS, Groom Q, Ort DR (2000) Differential effects of chilling-induced photooxidation on the redox regulation of photosynthetic enzymes. Biochemistry 39:6679–6688

Karimi M, Inzé D, Depicker A (2002) GATEWAY™ vectors for *Agrobacterium*-mediated plant transformation. Trends Plant Sci 7:193–195

Keown JR, Pearce FG (2014) Characterization of spinach Ribulose-1,5-bisphosphate carboxylase/oxygenase activase isoforms reveals hexameric assemblies with increased thermal stability. Biochem J 464:413–423

Kim K, Portis AR (2005) Temperature dependence of photosynthesis in *Arabidopsis* plants with modifications in Rubisco activase and membrane fluidity. Plant Cell Physiol 46:522–530

Kim SY, Harvey CM, Giese J, Lassowskat I, Singh V, Cavanagh AP, Spalding MH, Finkemeier I, Ort DR, Huber SC (2019) *In vivo* evidence for a regulatory role of phosphorylation of *Arabidopsis* Rubisco activase at the Thr78 site. Proc Natl Acad Sci 116:18723–18731

Kim SY, Slattery RA, Ort DR (2021) A role for differential Rubisco activase isoform expression in C4 bioenergy grasses at high temperature. GCB Bioenergy 13:211–223

Kromdijk J, Głowacka K, Leonelli L, Gabilly ST, Iwai M, Niyogi KK, Long SP (2016) Improving photosynthesis and crop productivity by accelerating recovery from photoprotection. Science 354:857–861

Kubien DS, Sage RF (2008) The temperature response of photosynthesis in tobacco with reduced amounts of Rubisco. Plant Cell Environ 31:407–418

Kunz C, Schöb H, Stam M, Kooter JM, Meins F (1996) Developmentally regulated silencing and reactivation of tobacco chitinase transgene expression. Plant J 10:437–450

Lawson T, Blatt MR (2014) Stomatal size, speed, and responsiveness impact on photosynthesis and water use efficiency. Plant Physiol 164:1556–1570

Lobo FA, Barros MP, Dalmagro HJ, Dalmolin ÂC, Pereira WE, Souza ÉC, Vourlitis GL, Ortíz CER (2013) Fitting net photosynthetic light-response curves with Microsoft Excel—a critical look at the models. Photosynthetica 51:445–456

Long SP, Bernacchi CJ (2003) Gas exchange measurements, what can they tell us about the underlying limitations to photosynthesis? Procedures and sources of error. J Exp Bot 54:2393–2401

Mate CJ, Hudson GS, von Caemmerer S, Evans JR, Andrews TJ (1993) Reduction of Ribulose-bisphosphate carboxylase activase levels in tobacco (*Nicotiana-tabacum*) by antisense RNA reduces Ribulose-bisphosphate carboxylase carbamylation and impairs photosynthesis. Plant Physiol 102:1119–1128

Mate CJ, von Caemmerer S, Evans JR, Hudson GS, Andrews TJ (1996) The relationship between CO_2-assimilation rate, Rubisco carbamylation and Rubisco activase content in activase-deficient transgenic tobacco suggests a simple model of activase action. Planta 198:604–613

Mott KA, Snyder GW, Woodrow IE (1997) Kinetics of Rubisco activation as determined from gas-exchange measurements in antisense plants of *Arabidopsis thaliana* containing reduced levels of Rubisco activase. Funct Plant Biol 24:811–818

Olascoaga B, Arthur AM, Atherton J, Porcar-Castell A (2016) A comparison of methods to estimate photosynthetic light absorption in leaves with contrasting morphology. Tree Physiol. https://doi.org/10.1093/treephys/tpv133

Orr DJ, Alcântara A, Kapralov MV, Andralojc PJ, Carmo-Silva AE, Parry MAJ (2016) Surveying Rubisco diversity and temperature response to improve crop photosynthetic efficiency. Plant Physiol 172:707–717

Ort DR, Merchant SS, Alric J, Barkan A, Blankenship RE, Bock R, Croce R, Hanson MR, Hibberd JM, Long SP et al (2015) Redesigning photosynthesis to sustainably meet global food and bioenergy demand. Proc Natl Acad Sci 112:8529–8536

Parry MAJ, Keys AJ, Madgwick PJ, Carmo-Silva AE, Andralojc PJ (2008) Rubisco regulation: a role for inhibitors. J Exp Bot 59:1569–1580

Paz MMM, Wang K (2009) Soybean transformation and regeneration using half-seed explant

Paz MM, Martinez JC, Kalvig AB, Fonger TM, Wang K (2006) Improved cotyledonary node method using an alternative explant derived from mature seed for efficient *Agrobacterium*-mediated soybean transformation. Plant Cell Rep 25:206–213

Perdomo JA, Degen GE, Worrall D, Carmo-Silva AE (2019) Rubisco activation by wheat Rubisco activase isoform 2β is insensitive to inhibition by ADP. Biochem J 476:2595–2606

Ristic Z, Momčilović I, Bukovnik U, Prasad PVV, Fu J, DeRidder BP, Elthon TE, Mladenov N (2009) Rubisco activase and wheat productivity under heat-stress conditions. J Exp Bot 60:4003–4014

Rundle SJ, Zielinski RE (1991) Organization and expression of two tandemly oriented genes encoding Ribulosebisphosphate carboxylase/oxygenase activase in barley. J Biol Chem 266:4677–4685

Sage RF, Way DA, Kubien DS (2008) Rubisco, Rubisco activase, and global climate change. J Exp Bot 59:1581–1595

Salvucci ME, DeRidder BP, Portis AR (2006) Effect of activase level and isoform on the thermotolerance of photosynthesis in *Arabidopsis*. J Exp Bot 57:3793–3799

Scafaro AP, Bautsoens N, den Boer B, Van Rie J, Gallé A (2019a) A conserved sequence from heat-adapted species improves Rubisco activase thermostability in wheat. Plant Physiol 181:43–54

Scafaro AP, Vleesschauwer DD, Bautsoens N, Hannah MA, den Boer B, Gallé A, Rie JV (2019b) A single point mutation in the C-terminal extension of wheat Rubisco activase dramatically reduces ADP inhibition via enhanced ATP binding affinity. J Biol Chem 294:17931–17940

Schrader SM, Kleinbeck KR, Sharkey TD (2007) Rapid heating of intact leaves reveals initial effects of stromal oxidation on photosynthesis. Plant Cell Environ 30:671–678

Sharkey TD, Zhang R (2010) High temperature effects on electron and proton circuits of photosynthesis. J Integr Plant Biol 52:712–722

Sharwood RE, Sonawane BV, Ghannoum O, Whitney SM (2016) Improved analysis of C_4 and C_3 photosynthesis via refined *in vitro* assays of their carbon fixation biochemistry. J Exp Bot 67:3137–3148

Shivhare D, Mueller-Cajar O (2017) *In vitro* characterization of thermostable CAM Rubisco activase reveals a Rubisco interacting surface loop. Plant Physiol 174:1505–1516

Shivhare D, Ng J, Tsai Y-CC, Mueller-Cajar O (2019) Probing the rice Rubisco-Rubisco activase interaction via subunit heterooligomerization. Proc Natl Acad Sci 116:24041–24048

Slattery RA, Walker BJ, Weber APM, Ort DR (2018) The impacts of fluctuating light on crop performance. Plant Physiol 176:990–1003

Soleh MA, Tanaka Y, Kim SY, Huber SC, Sakoda K, Shiraiwa T (2017) Identification of large variation in the photosynthetic induction response among 37 soybean [*Glycine max* (L.) Merr.] genotypes that is not correlated with steady-state photosynthetic capacity. Photosynth Res 131:305–315

Stotz M, Mueller-Cajar O, Ciniawsky S, Wendler P, Hartl FU, Bracher A, Hayer-Hartl M (2011) Structure of green-type Rubisco activase from tobacco. Nat Struct Mol Biol 18:1366–1370

Sukenik S, Ren P, Gruebele M (2017) Weak protein–protein interactions in live cells are quantified by cell-volume modulation. Proc Natl Acad Sci 114:6776–6781

Taylor SH, Long SP (2017) Slow induction of photosynthesis on shade to sun transitions in wheat may cost at least 21% of productivity. Philos Trans R Soc B Biol Sci. https://doi.org/10.1098/rstb.2016.0543

von Caemmerer S (2000) Biochemical models of leaf photosynthesis. Csiro Publishing, Collingwood

Walker B, Ariza LS, Kaines S, Badger MR, Cousins AB (2013) Temperature response of in vivo Rubisco kinetics and mesophyll conductance in *Arabidopsis thaliana*: comparisons to *Nicotiana tabacum*. Plant Cell Environ 36:2108–2119

Wang Y, Burgess SJ, de Becker EM, Long SP (2020) Photosynthesis in the fleeting shadows: an overlooked opportunity for increasing crop productivity? Plant J 101:874–884

Werneke JM, Chatfield JM, Ogren WL (1989) Alternative mRNA splicing generates the two Ribulosebisphosphate carboxylase/oxygenase activase polypeptides in spinach and *Arabidopsis*. Plant Cell 1:815–825

Wise RR, Olson AJ, Schrader SM, Sharkey TD (2004) Electron transport is the functional limitation of photosynthesis in field-grown pima cotton plants at high temperature. Plant Cell Environ 27:717–724

Woodrow IE, Mott KA (1989) Rate limitation of non-steady-state photosynthesis by Ribulose-1,5-bisphosphate carboxylase in spinach. Funct Plant Biol 16:487–500

Yamori W, von Caemmerer S (2009) Effect of Rubisco activase deficiency on the temperature response of CO_2 assimilation rate and Rubisco activation state: insights from transgenic tobacco with reduced amounts of Rubisco activase. Plant Physiol 151:2073–2082

Yokota A, Canvin DT (1985) Ribulose bisphosphate carboxylase/oxygenase content determined with [^{14}C]carboxypentitol bisphosphate in plants and algae. Plant Physiol 77:5

Yoshida K, Hara S, Hisabori T (2015) Thioredoxin selectivity for thiol-based redox regulation of target proteins in chloroplasts. J Biol Chem 290:14278–14288

Zhang Z, Komatsu S (2000) Molecular cloning and characterization of cDNAs encoding two isoforms of Ribulose-1,5-bisphosphate carboxylase/oxygenase activase in rice(*Oryza sativa* L.). J Biochem (tokyo) 128:383–389

Zhang N, Portis AR (1999) Mechanism of light regulation of Rubisco: a specific role for the larger Rubisco activase isoform involving reductive activation by thioredoxin-f. Proc Natl Acad Sci 96:9438–9443

Zhang M, Li X, Yang Y, Luo Z, Liu C, Gong M, Zou Z (2015) An acidified thermostabilizing mini-peptide derived from the carboxyl extension of the larger isoform of the plant Rubisco activase. J Biotechnol 212:116–124

Zhao G, Xu H, Zhang P, Su X, Zhao H (2017) Effects of 2,4-epibrassinolide on photosynthesis and Rubisco activase gene expression in *Triticum aestivum* L. seedlings under a combination of drought and heat stress. Plant Growth Regul 81:377–384

Zhong S-H, Liu J-Z, Jin H, Lin L, Li Q, Chen Y, Yuan Y-X, Wang Z-Y, Huang H, Qi Y-J et al (2013) Warm temperatures induce transgenerational epigenetic release of RNA silencing by inhibiting siRNA biogenesis in *Arabidopsis*. Proc Natl Acad Sci 110:9171–9176